

## Coloration and Ion Insertion Kinetics Study in Electrochromic WO<sub>3</sub> Films by Chronoamperometry

KaiLing Zhou, Hao Wang, and Jingbing Liu\*

The College of Materials Science and Engineering, Beijing University of Technology, Beijing 100124, China.

\*E-mail: [liujingbing@bjut.edu.cn](mailto:liujingbing@bjut.edu.cn)

Received: 5 April 2020 / Accepted: 22 May 2020 / Published: 10 July 2020

---

Devices relying on reversible ion intercalation are used in sustainable energy technology, for example, in batteries, in rechargeable electrical and electrochromic (EC) glazing for energy efficient buildings. Degradation of electrochromic thin films under extended charge insertion/extraction is a technologically important issue for which no in-depth understanding is currently available. The influence of coloration depth on the performance characteristics and lifetime of electrochromic WO<sub>3</sub> materials is investigated using chronoamperometry technology in this work. It is shown that depending on the cycling time, and the applied voltage, two different types of adsorption sites, viz. the shallow sites, surrounded by low-energy barriers and deep sites with high-energy barriers are created in the WO<sub>3</sub> host structures. During the bleaching process, higher cycling time and applied voltage create a large coloration depth leading to trapped immobile Li<sup>+</sup> ions hindering free ion transportation and subsequent degradation of electrochromic performance. This study offers a new understanding on the degradation mechanisms of the electrochromic materials and provides a general guideline suggesting the use of low voltage and cycling time for controlling the charge insertion and extraction in electrochromic materials by avoiding the large coloring depths.

---

**Keywords:** WO<sub>3</sub> film; Coloration Depth; Chronoamperometry Technology; Trapped ions

### 1. INTRODUCTION

The electrochromic (EC) phenomenon is considered to have reversible optical properties under the application of a voltage. The reversible electrochemical reactions change the reflectance, absorbance, and transmittance of the materials. [1] Electrochromic films have received more and more attention due to their promising applications in many fields (e.g., self-modified rear-view car mirrors and sun-protective smart windows). [2-5] Compared to polymer-based materials, metal oxide

electrochromic films show distinct advantages, including high thermal and mechanical stability.[6] Among these oxides, tungsten trioxide ( $\text{WO}_3$ ) is a promising electrochromic material and has been used in smart windows applications. [7]  $\text{WO}_3$  films appear deep-blue and colorless under the applications of negative and positive electrical fields, respectively. [8] In  $\text{Li}^+$  electrolyte, the electrochromic features of  $\text{WO}_3$  films are related to the insertion/extraction behavior of  $\text{Li}^+$  ions according to the following reaction:[9]



where  $x$  represents the mole fraction of inserted  $\text{Li}^+$  ions in the  $\text{WO}_3$  structure. Long-term durability of the electrochromic films is an essential requirement for optical modulation necessary for industrial applications. Under negative bias, the insertion of  $\text{Li}^+$  ions into the  $\text{WO}_3$  network results in a deep blue color response. Subsequently, under the application of a positive bias voltage, the  $\text{Li}^+$  ions get extracted out, and the color of  $\text{WO}_3$  films switches from dark blue to colorless. After the application of some voltage cycles, degradation in optical modulation properties of  $\text{WO}_3$  films is observed, [10, 11] as the inserted  $\text{Li}^+$  ions cannot be completely extracted out of  $\text{WO}_3$  films. [12, 13] Upon further voltage cycling, the trapped  $\text{Li}^+$  ions show gradual accumulation in the host structure, causing decay of the electrochromic performance. Granqvist et al. have reported two types of trap sites in  $\text{WO}_3$  host structures, include: “shallow trap sites” surrounded by low energy barrier and “deep trap sites” with high energy barrier. [14] When the  $\text{Li}^+$  ions diffuse into the shallow trap sites, the ions can be completely extracted out from the structure under the application of a reverse electric field. However, when the ions are driven into the deep trap sites, the inserted  $\text{Li}^+$  ions will be trapped and become immobile due to their high energy barrier. This contributes to the generation of irreversible  $\text{Li}^+$  ions in  $\text{WO}_3$  films. Although the trapped ions could be eliminated by constant-current-drive [15, 16], the formation mechanisms of trapped ions are still unclear. Some reports attribute the formation of trapped ions to the effects of the operating voltage range.[13, 17, 18] However, this is inclusive and the effects of trapped ions on the optical modulation ability and cycling lifetime of electrochromic  $\text{WO}_3$  films are still not clearly understood and need further attention.

As is well known, the charge/discharge depth of electrode materials in ion battery systems is related to its capacity fade, coulombic efficiency, and cycle life [19-21]. Especially, over-charge/discharge result in permanent internal damage, and irreversible changes in lifetime [22, 23]. Also, the influences of charge/discharge depth on the performance and lifetime of electrochromic materials have not yet been investigated. The coloration of  $\text{WO}_3$  is attributed to the simultaneous insertion of  $\text{Li}^+$  ions and electrons into the  $\text{WO}_3$  host structure. The inserted ions into the film take part in the coloration reaction. Thus the charge depth of electrode is related to the coloration depth. However, to the best of our knowledge, the effects of coloration depth and  $\text{Li}^+$  ion insertion on the performance of  $\text{WO}_3$  films have not yet been systematically studied.

Chronoamperometry is an efficient tool to explore the ion diffusion process in active electrodes.[24, 25] In this study, the effects of coloration depth on the trapped ion formation and degradation of  $\text{WO}_3$  film are explored via chronoamperometry technology with different duration cycling times of the potential in the coloration process. We have observed that the coloration depth has a crucial role on the electrochromic performance of  $\text{WO}_3$  films, and especially, the number of trapped ions in  $\text{WO}_3$  increases with the deepening of the coloring state resulting in a severe degradation after some cycles. The degradation mechanism is attributed to the over coloration depth resulting from a

long-time duration of potential. The inserted  $\text{Li}^+$  ions have enough energy to diffuse into 'deep' sites surrounded by a high-energy barrier in the  $\text{WO}_3$  host structure, resulting in immobile ions.

## 2. EXPERIMENTAL SECTION

### 2.1 Preparation of $\text{WO}_3$ thin film

The  $\text{WO}_3$  thin film electrodes were prepared by depositing  $\text{WO}_3$  thin films on the glass substrates pre-coated with ITO (indium tin oxide thin film) having a sheet resistivity of  $\sim 17$  ohm/sq. Before deposition, the ITO coated glass substrates were cleaned ultrasonically in deionized, alcohol, and then dried in the air atmosphere, respectively. Then, the  $\text{WO}_3$  films were deposited via a direct current magnetron sputtering system, in which a background pressure was set at  $2.0 \times 10^{-3}$  Pa. A metallic W target of 100 mm diameter was used. The distance between the target and substrate holder was about 7 cm, with an incident angle of  $41^\circ$ . Besides, the gas-flow rate of  $\text{O}_2/\text{Ar}$  was fixed at 9 sccm/27 sccm. During sputtering, the power on the target was set at 280 W, and the total pressure was maintained at about 2.2 Pa. All the films were prepared with a sputtering time of 20 mins at room temperature.

### 2.2 Electrochemical and optical measurements

The electrochemical performances of  $\text{WO}_3$  electrodes were measured in a three-electrode system, in which 1 M  $\text{LiClO}_4$  electrolyte prepared by dissolving lithium perchlorate into propylene carbonate. The  $\text{WO}_3$  film electrode was used as the working electrode. A platinum sheet and an  $\text{Ag}/\text{AgCl}$  electrode were used as the counter and the reference electrodes, respectively. For Chronoamperometry measurements, the applied voltage was set to +1 V to -1 V for different durations of 4 s, 8 s, 13 s, and 18 s, respectively, to explore the influence of coloration depth on the cycle life of  $\text{WO}_3$  film and trapped ions. The electrochemical measurements were carried out using electrochemical workstation (Model Princeton VersaSTAT 4). The transmittance of  $\text{WO}_3$  electrodes at 550 nm were observed via ultraviolet-visible-near-infrared spectrophotometer (Model Shimadzu UV-3101PC) during the electrochemical cycling tests.

## 3. RESULTS AND DISCUSSION

Chronoamperometry technology has been employed to estimate the response time and ion capacity of the electrochromic films [26-31]. In previous works, chronoamperometry technology has been applied to explore the electrochromic mechanism of  $\text{WO}_3$  and NiO films, demonstrating an extraordinary role of chronocoulometry in estimating the electrochromic performance and explaining the corresponding mechanisms [32]. Besides, the chronocoulometry technology has a distinct advantage of synchronously monitoring the ion charge density in the reaction process, compared to traditional cyclic voltammetry (CV). Moreover, chronoamperometry is a useful tool to investigate ion diffusion dynamics in electrodes [33, 34]. However, to the best of our knowledge, the coloration depth has not been comprehensively investigated for controlling the coloration potential signature in chronocoulometry technology. It is well known that the insertion of  $\text{Li}^+$  ions into the host structure

during the charging process results in the coloration process. However, during the discharging process, the inserted ions get extracted out of the film, leading to a bleaching response. In this study, the coloration depth of  $\text{WO}_3$  thin film is controlled by setting up different duration cycling time of the potential during the ions insertion process. In the three-electrode test system, the constant voltage discharge and charge processes can be achieved by employing double-potential step chronoamperometry technique. The response current as a function of time is recorded, and the current-time relationship is given by the Cottrell equation[35]:

$$i = nFA C_0 (D/\pi t)^{1/2} \quad (2)$$

where  $A$  represents the electrode area,  $F$  represents the Faraday constant, and  $C_0$  and  $D$  represent  $\text{Li}^+$  ion concentration in electrolyte and  $\text{Li}^+$  ion diffusion coefficient, respectively.

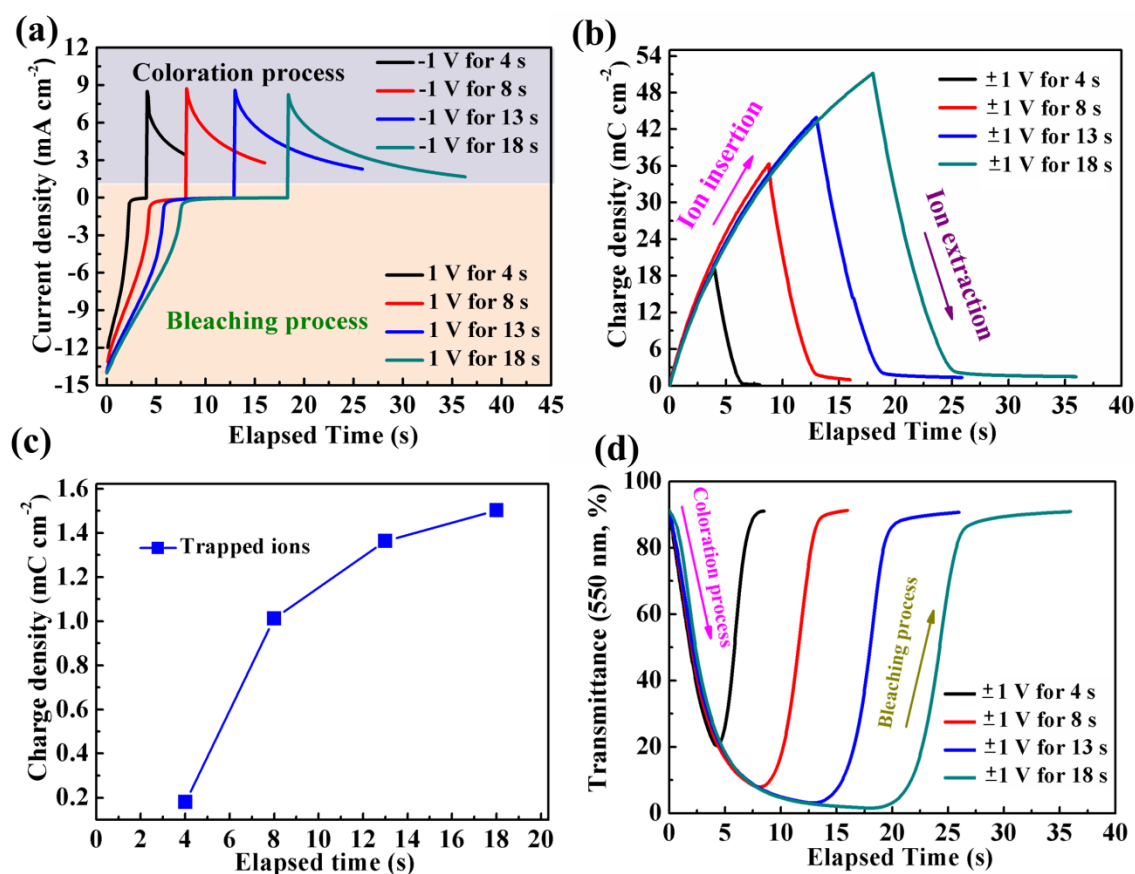


**Figure 1.** (a) Chronoamperometric curves of different potential duration time. (b) The charge-time curves during the chronoamperometric test. (c) The charge density of trapped ions in the  $\text{WO}_3$  host structure under different test conditions. (d) In-situ transmittance-time relationship at  $\lambda=550$  nm.

Figure 1(a) shows the current-time curves of the  $\text{WO}_3$  electrode under the double-step potential of -1 V to +1 V versus SCE (aturated silver chloride electrode) for different time steps of 4 s, 8 s, 13 s, and 18 s. For all the samples, the current density in the bleaching process could reach to zero while the coloration current density shows a constant value after the step time. It is because a large quantity of  $\text{WO}_3$  can react with the  $\text{Li}^+$  ions in the coloration process to produce  $\text{Li}_x\text{WO}_3$ , and eventually, the coloration reaction reaches a balanced state due to sufficient supply of ions in the  $\text{WO}_3$  sites. In the bleaching process, the resultant  $\text{Li}_x\text{WO}_3$  decompose to generate  $\text{WO}_3$ , and then the current density

reaches to zero value when the generated  $\text{Li}_x\text{WO}_3$  is completely decomposed,[36]. Besides, the current density during the bleaching process is larger than that of the coloration process, and the bleaching current shows a rapid decay. The coloration response time ( $t_c$ ) and bleaching response time ( $t_b$ ) are obtained by the current-time data as shown in Fig. 1(a). The bleaching response time is found to be faster when compared to the coloring process due to the higher conductivity of the tungsten bronze conductor ( $\text{Li}_x\text{WO}_3$ ) than that of insulator  $\text{WO}_3$ . [37]

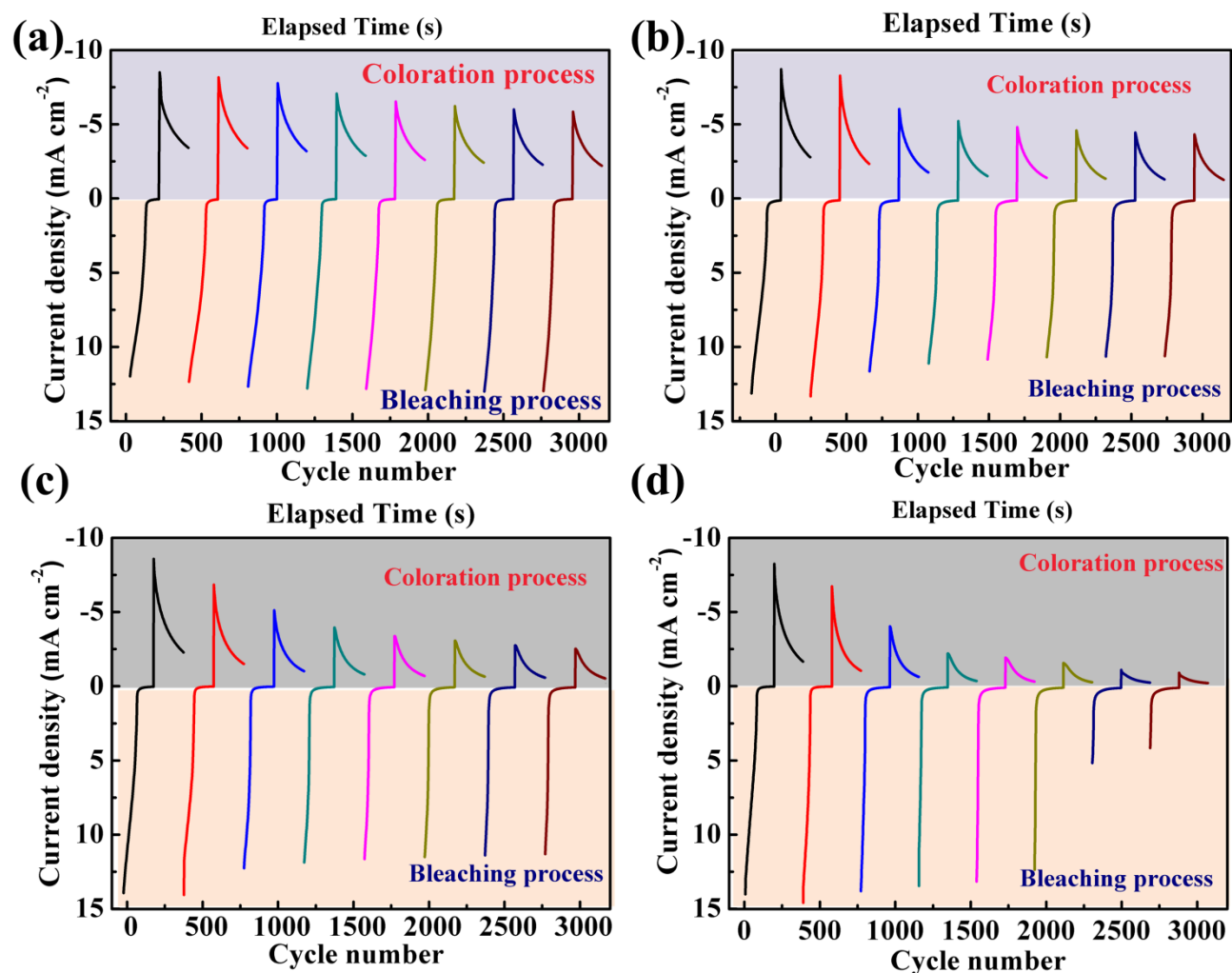


**Figure 2.** The evolutions of Chronoamperometry curves of  $\text{WO}_3$  film with a fixed coloring potential -1 V for different duration time of (a) 4 s, (b) 8 s, (c) 13 s, and (d) 18 s.

The charge density of  $\text{Li}^+$  ions involved in the coloring reaction is calculated by the corresponding current-time curve and can be expressed with the following equation:

$$Q = \int_0^t I dt = 2nFAD^{1/2}C_0\pi^{-1/2}t^{1/2} \quad (3)$$

where “ $Q$ ” represents the number of ions. As shown in Fig. 1b, the long-time potential duration will contribute more ions in the electrochromic reaction. Specifically, the inserted ions are  $19.15 \text{ mC cm}^{-2}$ ,  $36.38 \text{ mC cm}^{-2}$ ,  $43.96 \text{ mC cm}^{-2}$  and  $51.19 \text{ mC cm}^{-2}$  in the films with -1 V versus SCE for 4 s, 8 s, 13 s and 18 s, respectively. Besides, the charge densities do not return to zero during the ion extraction process, suggesting that a part of inserted  $\text{Li}^+$  ions have not extracted out of the  $\text{WO}_3$  film. These  $\text{Li}^+$  ions are defined as trapped ions, and the relationship between the quantity of trapped

$\text{Li}^+$  ions and duration time of potential is shown in Fig. 1(c), which suggests that the long-time application of the electrical field will result in the formation of more trapped  $\text{Li}^+$  ions in the film. Usually, the quantity of inserted  $\text{Li}^+$  ions determines the optical modulation property of electrochromic film films.

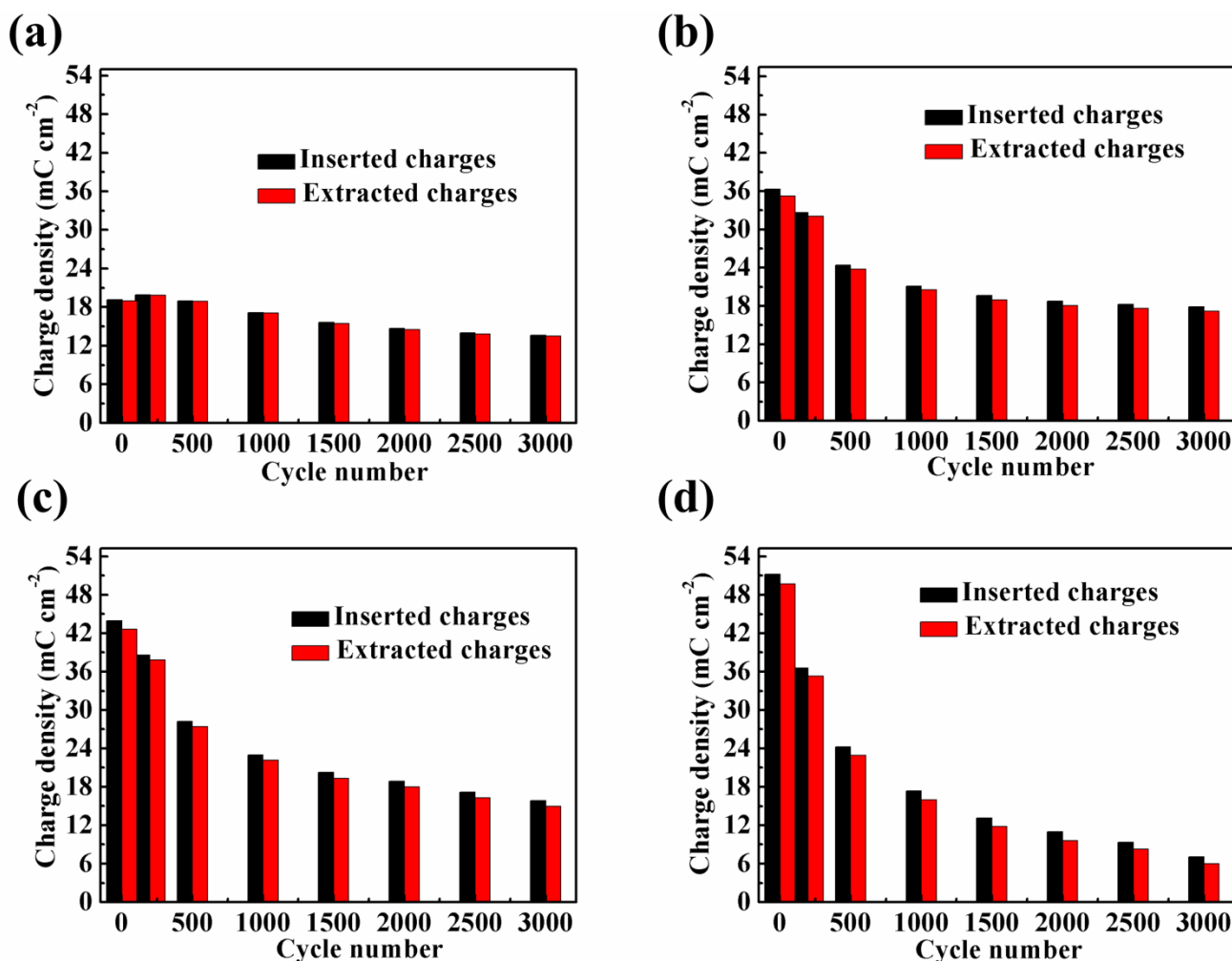


**Figure 3.** Evolution of the charge density of inserted and extracted  $\text{Li}^+$  ions in  $\text{WO}_3$  film under different coloring duration time of (a) 4 s, (b) 8 s, (c) 13 s, and (d) 18 s.

Figure 1(d) shows the recorded transmittance-time curves of  $\text{WO}_3$  films. The film films under the longest potential duration time of 18 s shows the lowest coloration depth of about 1.5% in optical transmittance and the largest optical modulation ability of about 89.7% as calculated from the difference between the bleaching transmittances and coloration transmittances. In the same way, the coloration transmittance of the  $\text{WO}_3$  film with 4 s, 8 s, and 13 s is 16.9%, 7.4%, and 2.9%, respectively. These results suggest that the  $\text{WO}_3$  films show various ion storage ability, optical modulation ability, and different quantity of trapped ions under the different coloration depths.

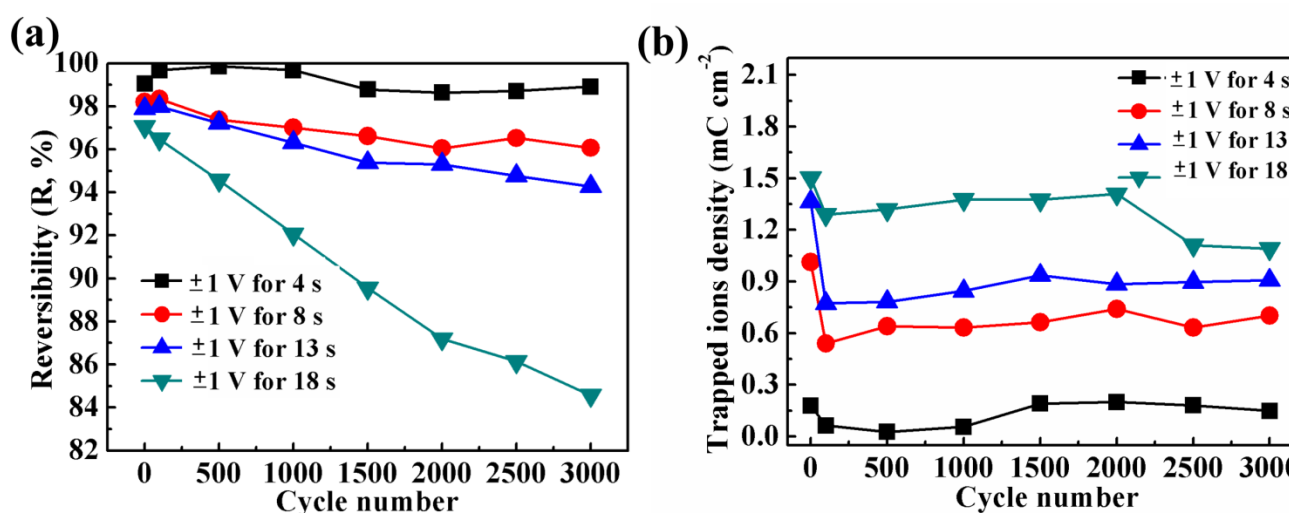


**Figure 4.** Cyclic evolution of (a) reversibility and (b) trapped ion density of the WO<sub>3</sub> films under different coloring time of 4 s, 8 s, 13 s, and 18 s.

The performance of the electrochromic WO<sub>3</sub> films usually suffer degradation mentioned above when the trapped Li<sup>+</sup> ions accumulate in the host structure. The above results demonstrate that the formation of trapped ions in WO<sub>3</sub> films is affected by the coloration depth. It is necessary to study the multi-cyclic performance of the electrode under the different coloration depth to analyze the decay mechanism. As shown in Fig. 2, the WO<sub>3</sub> films exhibit different cyclic stabilities under different coloration depth. Mainly, the WO<sub>3</sub> film under a coloration time of 4 s exhibits the highest cyclic stability (Fig. 2a). The current density and peak shape show inconspicuous change during 3000 cycles. When the duration time of the potential increase to 8 s, the stability of the WO<sub>3</sub> film shows some decrease ( Fig. 2b). Further, the film shows obvious degradation when the duration time of the potential increase to 18 s ( Fig. 2d). The current density also decreases to almost zero value after 3000 cycles, indicating a weak electrochromic activity of the WO<sub>3</sub> electrode.

The electrochromic stability could further be explored by the corresponding cycling evolution of ion charge density calculated by equation (3). As expected, the relationship between duration time of potential and stability of charge capacity is consistent with the current density evolution. Mainly, for the step potential of -1 V for 4 s, the charge density exhibits the highest stability, and, not much decay could be observed, as shown in Fig. 3(a). When the duration time of the potential increases to 8 s, the charge capacity shows some degradation. Further, this trend is magnified by increasing the duration time to 18 s ( Fig. 3d). The film shows a larger ion capacity at the initial few cycles, then gradually decreases and finally gets close to zero upon further cycling. These results indicate that the coloration depth significantly affect the ion storage capacity of WO<sub>3</sub> films. Also, the inserted charge density shows some difference with the extracted charge density, suggesting the irreversible accumulation of inserted Li<sup>+</sup> ions in the film.

Usually, the electrochromic films with high stability should prohibit the accumulation of irreversible ions in the films. As mentioned above, the formation of the trapped ions due to inserted ions, are difficult to extract out of the films in the subsequent bleaching process. The amount of the trapped ions ( $Q_{\text{trap}}$ ) can be calculated as follows:

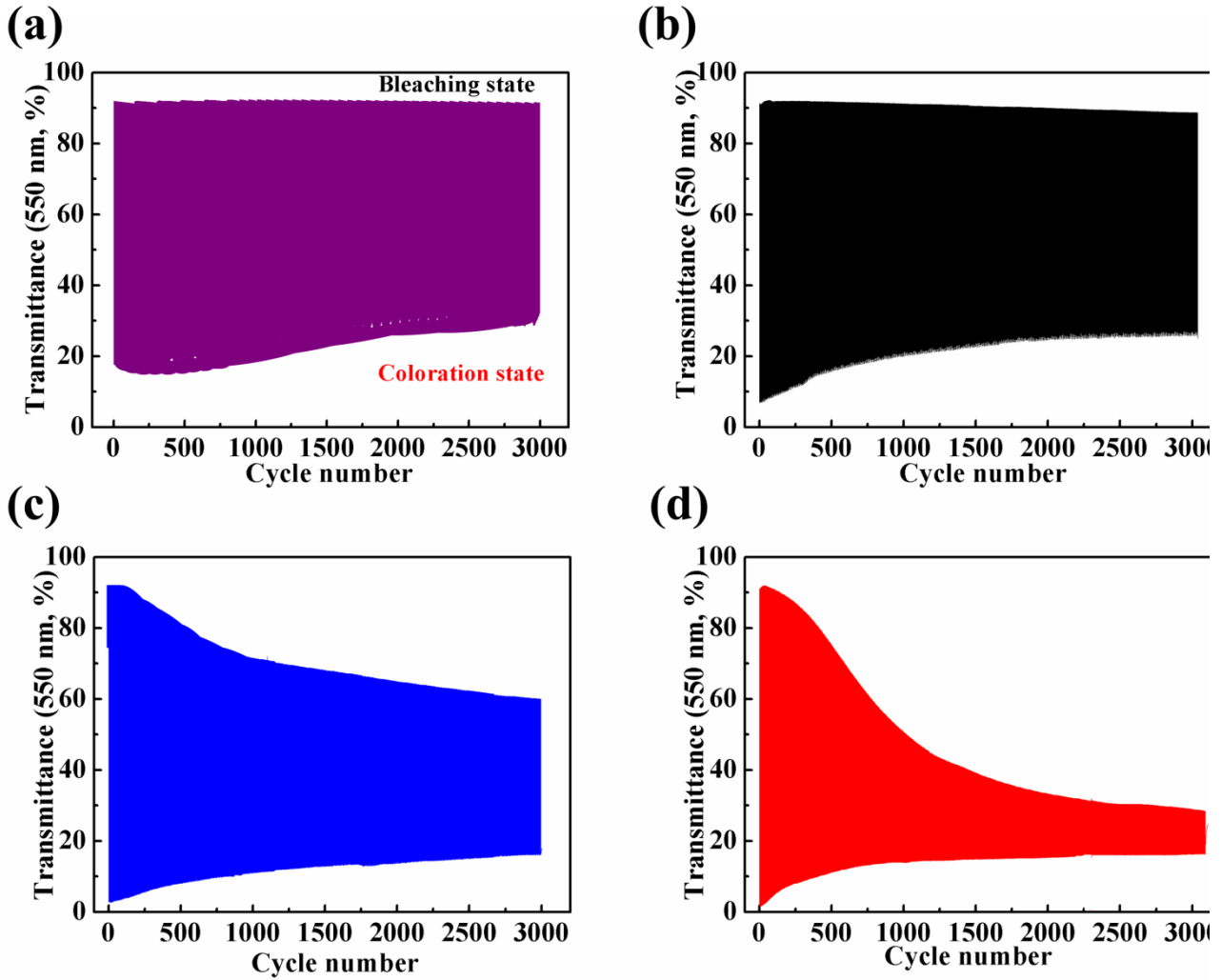


**Figure 5.** (a) Multi-cyclic transmittance-time curves of  $\text{WO}_3$  film at  $\lambda=550$  nm under a fixed coloring potential  $-1$  V for different duration time of (a) 4 s, (b) 8 s, (c) 13 s and (d) 18 s.

$$Q_{\text{ui}} = \int_1^m \{(1 - R) \times Q_{\text{in}}\} dn \quad (4)$$

where  $m$  is the cycle number,  $Q_{\text{ui}}$  is the accumulated quantity of “trapped ion” at the  $m$ -th cycle. The reversibility  $R$  is estimated by the ratio of extracted charge ( $Q_{\text{ex}}$ ) to inserted charge ( $Q_{\text{in}}$ ) during the reaction process[38]:

$$R = \frac{Q_{\text{ex}}}{Q_{\text{in}}} \times 100\% \quad (5)$$

The  $Q_{\text{trap}}$  is determined from the amount of inserted ions  $Q_{\text{in}}$  and the reversibility  $R$ . In Fig 4 (a), the  $R$  of  $\text{WO}_3$  film under the long potential duration time is lower than that of the sample with short potential duration time at the same cycle, and the corresponding  $Q_{\text{in}}$  shows a larger value. Consequently, the amount of “trapped  $\text{Li}^+$  ions” increases with longer duration time of potential, as shown in Fig. 4 (b).

$\text{Li}^+$  ion insertion in  $\text{WO}_3$  films will result in a color change of the film from colorless to deep-blue. In the bleaching process,  $\text{Li}^+$  ions will get extracted from the  $\text{WO}_3$  host structure. The evolution of transmittance-time curves of the film is recorded during cycling, as shown in Fig. 5. Downward optical transmittance curves and negative current responses are obtained when a negative potential is applied to the film electrode during the coloration process. Upward optical transmittance curves, as well as positive current curves, are obtained during the bleaching process when positive potential is

applied to the film. As shown in Figs. 5(a-b), the coloration state shows no obvious degradation, and the bleaching state remains stable during all the cycles, suggest excellent stability in optical modulation. However, under the long potential times, of 13 s and 18 s as shown in Figs. 5(c-d), the transmittance of WO<sub>3</sub> film at bleaching state shows a significant decay than the coloration state.

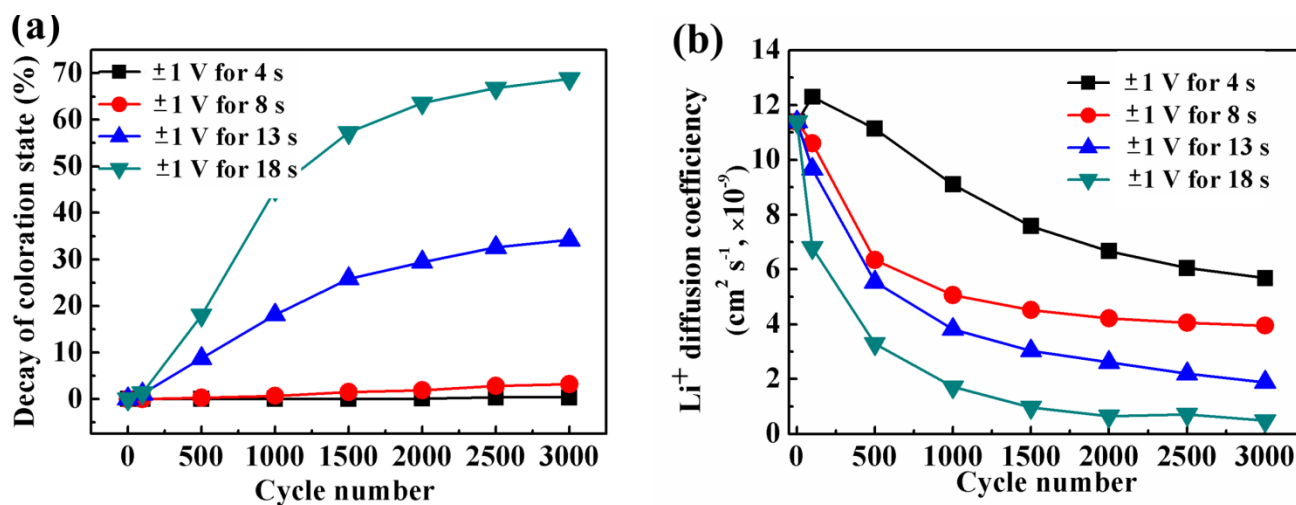


**Figure 6.** (a) Transmittance cyclic evolution of the film at coloration state and (b) calculated Li<sup>+</sup> ions diffusion coefficient change of WO<sub>3</sub> upon cycling under different test conditions.

The cyclic evolution of the optical transmittance of WO<sub>3</sub> films is shown in Fig. 6(a). These results suggest that the degradation of WO<sub>3</sub> electrochromic performance derives from the decay of bleaching state under long potential durability for 13 s and 18 s. As discussed above, the coloration process of WO<sub>3</sub> films corresponds to the Li<sup>+</sup> ion insertion process:  $\text{WO}_3 + x(\text{Li}^+ + \text{e}^-) \rightarrow \text{Li}_x\text{WO}_3$ , and the bleaching process corresponds to  $\text{Li}_x\text{WO}_3 \rightarrow \text{WO}_3 + x(\text{Li}^+ + \text{e}^-)$ . The formation of Li<sub>x</sub>WO<sub>3</sub> causes a decrease in transmittance. Therefore, the transmittance decay of the films during the bleaching state cycling for 13 s and 18 s samples should be attributed to the incomplete decomposition of Li<sub>x</sub>WO<sub>3</sub> during the extraction process. The incomplete decomposition of Li<sub>x</sub>WO<sub>3</sub> is due to the formation of “trapped ions” which is consistent with the earlier observations (see Fig. 4 b). Based on these results, the stability of WO<sub>3</sub> electrodes and the formation of trapped ions show a direct relationship to the coloration depth. To explore further on the degradation mechanisms, the diffusion coefficients of Li<sup>+</sup> ions are calculated using the equation (3) and are shown in Fig. 6 b. The films under a long potential durations of 13 s and 18 s show a large decay in ion diffusion after some cycles, and Li<sup>+</sup> ions can not diffuse into the film, suggesting that the Li<sup>+</sup> ions may be driven into the isolated ‘deep’ trap sites due to the high-energy under a long-time potential duration.

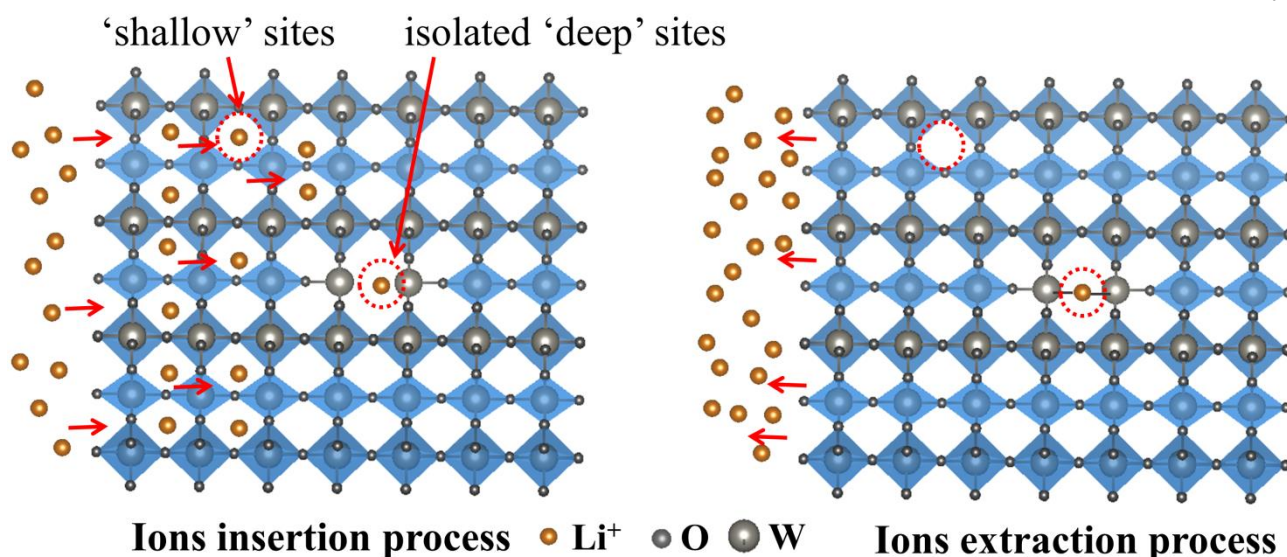


**Figure 7.** Simple schematic diagram of the formation mechanism of trapped ions in the  $\text{WO}_3$  host structure with large coloration depth.

A schematic diagram of the formation of trapped ions in the  $\text{WO}_3$  host structure with considerable coloration depth is shown in Fig. 7. As mentioned above, the  $\text{WO}_3$  host structure has two types of  $\text{Li}^+$  ions adsorption sites: (1) shallow reaction sites surrounded by low-energy barriers which allow ions to reversibly transport throughout the film; and (2) deep sites with high-energy barriers, in which ions become immobile once trapped. The large coloration depth obtained from the long-time potential duration in the ion insertion process provide enough energy for the  $\text{Li}^+$  ions to reach the ion trapped deep sites with a high energy barrier, resulting in the formation of immobile trapped ions in  $\text{WO}_3$  films (Figure 7). During the ion extraction process, trapped  $\text{Li}^+$  ions could not be extracted out of the  $\text{WO}_3$  films accumulate in the film. No doubt, these trapped ions will further hinder ion transportation, reduce the charge capacity and optical modulation ability of the  $\text{WO}_3$  films. Thus, it is better to avoid the high-energy ion diffusion process in inorganic electrochromic materials.

#### 4. CONCLUSION

In this study, the degradation mechanisms of electrochromic  $\text{WO}_3$  films were explored from different coloration depths measured using double-step chronoamperometry technology combined with an in-situ spectroelectrochemical measurement setup. It is observed that the long potential duration time will cause a considerable coloration depth and the formation of trapped ions in the  $\text{WO}_3$  host structure, being the main reason for the degradation of electrochromic performance. Due to  $\text{Li}^+$  ion diffusion, two different types of adsorption sites are generated: the shallow sites and deep sites, surrounded by low-energy and high-energy barriers, respectively, resulting in different coloration depths. Especially, large coloration depths due to long potential duration time will supply enough energy to drive the  $\text{Li}^+$  ions into the ‘deep’ sites with high-energy barriers, resulting in the formation of immobile trapped ions. Further, the formation of trapped  $\text{Li}^+$  ions in the  $\text{WO}_3$  host structures lead to decay of the bleaching state and trapped ions will hinder free ion transportation. As a result, the

quantity of inserted Li<sup>+</sup> ions into WO<sub>3</sub> films will decay upon cycling, resulting in the reduction of the coloration component (Li<sub>x</sub>WO<sub>3</sub>). Finally, electrochromic performance of WO<sub>3</sub> films degrade. This study leads to a new understanding of the degradation mechanisms of the electrochromic materials under different coloration depths and suggests one to avoid high-energy ions diffusion process in inorganic electrochromic materials by reducing the potential duration time.

#### ACKNOWLEDGMENTS

This work was supported by Beijing Natural Science Foundation (2161001).

#### References

1. P. M. Monk, R. J. Mortimer and D. R. Rosseinsky, *Electrochromism: fundamentals and applications*, John Wiley & Sons (2008).
2. D. R. Rosseinsky and R. J. Mortimer, *Adv. Mater.*, 13 (2001) 783.
3. G. Cai, P. Darmawan, M. Cui, J. Wang, J. Chen, S. Magdassi and P. S. Lee, *Adv. Energy Mater.*, 6 (2016) 1501882.
4. H. Li, J. Li, C. Hou, D. Ho, Q. Zhang, Y. Li and H. Wang, *Adv. Mater. Technologies*, 2 (2017) 1700047.
5. T. Y. Yun, X. Li, S. H. Kim and H. C. Moon, *ACS Appl. Mater. Interfaces*, 10 (2018) 43993.
6. T. Brezesinski, D. Fattakhova Rohlfing, S. Sallard, M. Antonietti and B. M. Smarsly, *Small*, 2 (2006) 1203.
7. F. Fabregat-Santiago, G. Garcia-Belmonte, J. Bisquert, N. S. Ferriols, P. R. Bueno, E. Longo, J. S. Antón and S. Castro-García, *J. Electrochem. Soc.*, 148 (2001) E302.
8. J. Wang, E. Khoo, P. S. Lee and J. Ma, *J. Phys. Chem. C*, 113 (2009) 9655.
9. O. Bohnke, C. Bohnke, G. Robert and B. Carquille, *Solid State Ionics*, 6 (1982) 121.
10. X. Tang, G. Chen, H. Liao, Z. Li, J. Zhang and J. Luo, *Electrochim. Acta*, 329 (2020) 135182.
11. E. Hopmann and A. Y. Elezzabi, *ACS Appl. Mater. Interfaces* 12 (2020) 1930.
12. S. Hashimoto and H. Matsuoka, *J. Electrochem. Soc.*, 138 (1991) 2403.
13. S. Hashimoto and H. Matsuoka, *Surf. Interface Anal.*, 19 (1992) 464.
14. R.T. Wen, C. G. Granqvist and G. A. Niklasson, *Nat. Mater.*, 14 (2015) 996.
15. M. A. Arvizu, R.T. Wen, D. Primetzhofer, J. E. Klemberg-Sapieha, L. Martinu, G. A. Niklasson and C. G. Granqvist, *ACS Appl. Mater. Interfaces*, 7 (2015) 26387.
16. B. Baloukas, M. A. Arvizu, R.-T. Wen, G. A. Niklasson, C. G. Granqvist, R. Vernhes, J. E. Klemberg-Sapieha and L. Martinu, *ACS Appl. Mater. Interfaces*, 9 (2017) 16995.
17. C. G. Granqvist, *Handbook of Inorganic Electrochromic Materials*, Elsevier (1995).
18. M. A. Arvizu, C. A. Triana, B. I. Stefanov, C.G. Granqvist and G. A. Niklasson, *Sol. Energy Mater. Sol. Cells*, 125 (2014) 184.
19. D. Marmorstein, T. H. Yu and K. A. Striebel, *J. Power Sources*, 89 (2000) 219.
20. N. Gang, R. E. White and B. N. Popov, *Electrochim. Acta*, 51 (2006) 2012.
21. S. S. Choi and S. L. Hong, *J. Power Sources*, 111 (2002) 130.
22. J. Garche, A. Jossen and H. Döring, *J. Power Sources*, 67 (1997) 201.
23. J. Kim, S. Lee and B. H. Cho, *J. Power Sources*, 196 (2011) 2227.
24. H. Lindström, S. Södergren, A. Solbrand, H. Rensmo, J. Hjelm, A. Hagfeldt and S.E. Lindquist, *J. Phys. Chem. B*, 101 (1997) 7710.
25. H.I. Yoo, J.K. Kim and C.E. Lee, *J. Electrochem. Soc.*, 156 (2009) B66.
26. J.H. Zhang, G.F. Cai, D. Zhou, H. Tang, X.L. Wang, C.D. Gu and J.P. Tu, *J. Mater. Chem. C*, 2 (2014) 7013.

27. B. Xu, L. Xu, G. Gao, W. Guo and S. Liu, *J. Colloid Interface Sci.*, 330 (2009) 408.
28. K. Nomura, K. Hirayama, T. Ohsaka, M. Nakanishi, O. Hatozaki and N. Oyama, *J. Macromolecular Sci.—Chem.*, 26 (1989) 593.
29. S. H. Mujawar, A. I. Inamdar, C. A. Betty, V. Ganesan and P. S. Patil, *Electrochim. Acta*, 52 (2007) 4899.
30. M. Mihelčič, I. Jerman, F. Švegl, A. Šurca Vuk, L. Slemenik Perše, J. Kovač, B. Orel and U. Posset, *Sol. Energy Mater. Sol. Cells*, 107 (2012) 175.
31. S. H. Mujawar, A. I. Inamdar, C. A. Betty, R. Cerc Korošec and P. S. Patil, *J. Appl. Electrochem.*, 41 (2010) 397.
32. K. Zhou, H. Wang, Y. Zhang, J. Liu and H. Yan, *J. Electrochem. Soc.*, 163 (2016) H1033.
33. H. Lindström, S. Södergren, A. Solbrand, H. Rensmo, J. Hjelm, A. Hagfeldt and S. E. Lindquist, *J. Phys. Chem. B*, 101 (1997) 7710.
34. J. Liu and A. Manthiram, *J. Electrochem. Soc.*, 156 (2009) B66.
35. M. D. Hawley and S. W. Feldberg, *J. Phys. Chem.*, 70 (1966) 3459.
36. K. Zhou, H. Wang, Y. Zhang, J. Liu and H. Yan, *Electroanalysis*, 29 (2017) 1573.
37. S. R. Bathe and P. Patil, *Sol. Energy Mater. Sol. Cells*, 91 (2007) 1097.
38. V. V. Kondalkar, P. B. Patil, R. M. Mane, P. S. Patil, S. Choudhury and P. N. Bhosal, *Macromol. Symp.*, 361 (2016) 47.

© 2020 The Authors. Published by ESG ([www.electrochemsci.org](http://www.electrochemsci.org)). This article is an open access article distributed under the terms and conditions of the Creative Commons Attribution license (<http://creativecommons.org/licenses/by/4.0/>).